

CHAPTER ONE HUNDRED FIFTY SIX

SCALE EFFECTS IN LARGE COASTAL MOBILE BED MODELS

J.W. Kamphuis* and R.B. Nairn*

ABSTRACT:

A series of mobile bed model tests of a prototype circular sand island was performed to determine scale effects. It was found that scale effect was largely a function of mobility number with some secondary effects of Reynolds number, bedform and critical profile depth. It was concluded that a model series using prototype sand grain size is necessary at this time to effect successful extrapolation to prototype.

1.0 INTRODUCTION

An extensive series of model tests was performed with circular islands consisting of sand only. The prototype modelled was an artificial island used for drilling purposes in the Canadian Beaufort Sea. It was located in 20 m of water, had a composite slope (mostly 1:12), a drilling platform of 50 m radius and nominally contained $5 \times 10^6 \text{ m}^3$ of 0.2 mm diameter sand. (Figures 1 and 2 show the model basin and the prototype island profile.) To date 30 different mobile bed models have been built and tested, using scales of 50, 75, 100 and 200 and sand particle sizes of 0.56, 0.18, 0.17 and 0.105 mm. The island models were tested until they were completely submerged.

Erosion volumes were measured at prototype time intervals of 3, 12, 36, 108 and 216 hours, based on hydrodynamic scaling (Froude) relationships. Progression of erosion was also monitored by recording the time to reach several benchmark stations. These were the leading edge of the drilling platform, a post located at the centre of the island, the trailing edge of the platform and the disappearance of the island underwater. Erosion volume was also measured when the test reached the post and when the island became submerged. Thus, erosion rates could be calculated for particular prototype time intervals as well as over the morphological time interval required for erosion to reach the post and for the island to become submerged. In the present paper erosion volumes on the front half of the island only are considered in the analysis.

* Department of Civil Engineering, Queen's University,
Kingston, Canada, K7L 3N6

The prototype wave climate was simulated using 8 second monochromatic waves arriving from one single direction. Each model was built twice. One model was subjected to a wave height of 6.5 m, while the other was tested at a wave height of 4.75 m. Both of these are considered to be extreme storm wave conditions. Several models were built more than twice for replication of results, removal of testing errors and for tests with different wave heights.

This paper presents a description of how a series of model tests should be performed and interpreted. This study differs from previous scale effects investigations because a strong longshore sand transport gradient exists in this truly three dimensional problem.

2.0 DIMENSIONAL ANALYSIS

The primary objective of coastal mobile bed modeling is to determine prototype sediment transport rates and morphology. A functional relationship between sediment transport and its parameters may be postulated as follows:

$$Q = f(H, L \text{ or } T, D \text{ or } m, \rho, \rho_s, g, \lambda, \nu) \quad [2.1]$$

Here Q is defined as the volumetric rate of sediment transport. The wave is described by the wave height H at the toe of the structure and wavelength L which is a function of wave period T . Many authors have shown beach slope m is related to grain diameter D , therefore D and m are not independent parameters. The median grain diameter D is retained since it was varied in the tests. The geometric parameter λ describes the actual physical size of the model island, for instance the diameter of island. Time t should be included as a characteristic parameter but since the tests were carried out for distinct prototype time periods (e.g. 0 to 3 hrs. or time for erosion to reach the post) each test can be viewed separately, initially neglecting time effects.

The island tests were performed for storm conditions with plunging breakers which produce much suspended load. Under these conditions bed load moved by shear stress under unbroken waves does not amount to a significant proportion of the sediment transport and hence in the present tests, as well as in the prototype, sediment transport is mainly a result of suspended sediment movement in the surf zone. Since surf zone phenomena are characterized by rough turbulent flow it might be postulated that viscosity should not be included in Equation 2.1. However, as shown in sections 4.2 and 4.4 the morphology of the eroded form of the island is related to viscosity and hence it must be retained as a parameter. The dimensionless relationship for volumetric sediment transport rate Q , may be written as

$$\frac{Q}{H^3/T} = \phi \left(\frac{gH^2 D^2}{L\nu^2}, \frac{H^2}{DL}, \frac{H}{L}, \frac{\lambda}{L}, \frac{\rho_s}{\rho} \right) \quad [2.2]$$

The influence of ρ_s/ρ has been discussed earlier - Kamphuis (1975a, 1982) and as a result all our coastal models use sand as a mobile bed material. Thus the influence of ρ_s/ρ was not tested in this series and ρ_s/ρ was kept the same as in the prototype. The island size λ/L was also kept constant and equal to the prototype value throughout these tests. Wave steepness H/L was varied in these tests, but in a geometrically similar model this ratio will also be the same as in the prototype.

This leaves the first two parameters which by virtue of the grain size D cannot be modelled correctly. Thus, these two parameters introduce scale effect. The first parameter is essentially a grain size Reynolds number, expressed in terms of the common wave parameters; the second is a mobility number or Shields parameter. The Reynolds number describes the boundary layer regime. The mobility number represents the ratio of inertia (or disturbing) forces to gravity (or restoring) forces and reflects actual amounts of sediment in motion as well as proportion of sediment in suspension. As scale decreases (larger models), the wave height increases and hence the Reynolds number and the mobility number will both increase resulting in more sediment movement and a larger proportion of material travelling in suspension.

3.0 MORPHOLOGICAL DEVELOPMENT

3.1 Description of Morphology

All the island tests with monochromatic waves featured a similar pattern of morphological development. Throughout the tests, the incident waves formed plunging breakers in the vicinity of the radial facing directly into the waves. In most tests sediment agitation and suspension was observed beneath the plunging breakers within the surf zone. Strong longshore currents developed alongside the island forming a longshore trench. The current carried suspended sediment from the zone of plunging breakers and deposited it to form symmetrical wing bars extending out from either side of the back of the island (Figure 3).

Large unidirectional flow dunes clearly defined the location of the longshore current. These dunes abruptly changed to wave induced ripples just outside the breaker line. From the bedform it was apparent that the point of maximum longshore current closely coincided with the zone of greatest bed agitation. This supposition was confirmed with current velocity measurements.

3.2 Rate of Morphological Development

Figure 4A shows cumulative erosion with time for one island test. It reveals that the erosion rate decreases with time as the island approaches dynamic equilibrium form or shape of minimum entropy. Replotting Figure 4A on a log scale as was done in Figure 4B shows a definite change in erosion rate when the leading edge of the erosion scarp infringes on the horizontal drilling platform.

During the erosion process, the waves on the front of the island tend to form an eroding profile which has a relatively constant shape and exhibits a critical depth below which no erosion takes place. The eroding profile has been fully formed at about the time that the erosion reaches the horizontal platform, hence the sudden decrease in erosion rate in Figure 4B. After that time the profile simply erodes back into the island as shown in Figure 5 but since the island is circular, there will be less and less material to erode as the profile approaches the centre of the island. This is reflected in the continuing decrease in erosion rate in Figure 4.

4.0 DIAMETER EFFECTS

The inability to model grain size correctly in the model introduces scale effects as described in Section 2 which may be classified as Inertial Effects (incorrect mobility number) and Viscous Effects (incorrect Reynolds number).

4.1 Inertial Effects

Dimensionless erosion rate is plotted as a function of the mobility number H^2/DL in Figures 6 and 7. If there were no scale effect, all points for constant sediment size and wave conditions would lie on a horizontal line. If the scale effect were purely a function of H^2/DL , Figures 6 and 7 would show a straight line. In fact, the lines are curved, indicating that scale effect is largely a function of H^2/DL but is also influenced by the other parameters. Since ρ/ρ and λ/L were not varied and since along any line in Figures 6 and 7 H/L is constant, the curvature must be a function of the Reynolds number gH^2D^2/Lv^2 . It may be seen in Figure 6 which shows erosion at constant (prototype) time using Froude scaling that as time increases, the curvature of the lines also increases, i.e. there are some secondary considerations. These may be explained directly from Figures 4 and 5. Smaller scale models are at a further state of erosion than larger scale models at any fixed time. This means the average erosion rate over such a period is less as may be inferred from Figure 4. Also the erosion rate is decreased because the constant eroding profile has progressed further into the island for these smaller scale tests, leaving less material to erode.

The latter two effects which may be called "time effects" can be removed by plotting erosion rate for a certain stage of morphological development as was done in Figure 7 where the average erosion rate to the post is plotted. This figure shows less curvature than Figure 6 and essentially the curvature is a result of viscous or Reynolds Number (gH^2D^2/Lv^2) effect which is examined further in the next section.

Another way to investigate the effect of the mobility number on island erosion is to plot the time it takes to erode to a certain morphological stage. Figure 8 shows the time required to erode to the post. Once again it is seen that the lines for constant grain size are not straight but curved, reflecting the effect of viscosity.

One reason that sediment transport is highly dependent on mobility number is the fact that the amount of suspended load is closely related to mobility number. Sawaragi and Deguchi (1978) suggest criteria based on the dimensionless parameter H/D to distinguish between prominence of bed load versus suspended load.

$H/D < 125$	no suspension
$H/D > 200$	sediment is suspended (transition)
$H/D > 300$	suspended load exceeds bed load

The H/D parameter is identical to H^2/DL if the model is geometrically similar (then H/L will be the same in model and prototype). In the island tests H/D was greater than 300 in most of the finer sand tests (0.105 mm and 0.18 mm) indicating prevalent suspended load. The coarse 0.56 mm sand at all scales and the finer sands at 200 scale were transported almost entirely by bed load, quite unlike the transport mechanism in prototype. The modeling of prototype wave conditions which produce suspended load using typical model scales of 200 to 50 must therefore be performed with a model grain size smaller than 0.2 mm to 0.3 mm ($H/D > 300$) to ensure suspended load is prevalent in the model.

4.2 Viscous Effects

The effects of viscosity are not negligible as often assumed in coastal mobile bed modeling. Because of the flow reversals in wave mechanics often the flow regime in the boundary layer is smooth especially outside the breaking zone. Viscosity effects complicate the analysis in several ways.

Preliminary analysis indicated that the sediment transport increased with an increase in the grain diameter from 0.18 mm to 0.56 mm. It was shown in the previous chapter that bed load is dominant in this grain size range for the scales tested. In order to offer an explanation for this strange variation in sediment transport the boundary layer regime outside the surf zone must be examined. The Shields diagram for unidirectional flow shows that grains become increasingly mobile as the grain size increases from 0.2 mm to 0.6 mm (see Figure 9). This is the region of transition from laminar to turbulent flow in the boundary layer. In this region an increase in grain size intensifies the turbulence within the boundary layer which induces greater sediment mobility. For grain diameters greater than 0.6 mm (for unidirectional flow) the boundary layer flow is fully developed rough turbulent and increases in grain diameter do not cause further increases in sediment mobility. This same phenomenon exists for oscillatory fluid motion. When the island tests with the finer sands are plotted on the flow regime diagram developed by Kamphuis (1975), they indicate smooth flow in the boundary layer which is either laminar or in transition to turbulent. The coarser sand is in the transition region to rough turbulent (see Figure 10), and for the range of scales tested the flow in the boundary layer will be in transition for grain sizes between 0.3 and 4.5 mm. Within this transition zone an increase in grain diameter causes an increase in sediment mobility which translates to greater sediment transport

rates. Similar transition ranges have been suggested by Komar and Miller (1974) and Madsen and Grant (1976).

As the grain size Reynolds number, gH^2D^2/Lv^2 becomes large the boundary layer will become turbulent and the effects of viscosity on bed load may be expected to become negligible. In Figures 7 and 8 there is less curvature through data points corresponding to the tests with smaller scales indicating a reduction in the Reynolds number effect. The remaining curvature is attributable to both remaining Reynolds number effect and secondary influences such as bedform and critical depth.

4.3 Bedform Effect

In the tests with smaller scales and for the two finer sands the existence of bedform indicates that the boundary layer flow is rough turbulent and therefore the effects of viscosity should be minimal. The remaining curvature in Figures 7 and 8 may in part be attributable to bedform since it is a function of the ratio of orbital amplitude to grain diameter which varies with scale. While a varying size of bedform is present in the models, it will be different from the prototype, resulting in scale effect; in fact it is probable that in the prototype under the wave conditions being tested all bedform will be washed out.

The significance of this scale effect may be limited since it has been estimated that the wave energy loss due to the large turbulence brought into the water from the surface by the breaking wave was some hundred times the amount of energy dissipated due to bottom shear stress - (Sawaragi et al (1974)).

4.4 Critical Depth Effect

The critical depth scale effect is important because it has a large impact on the amount of material eroded. Because of the measuring techniques adopted it was difficult to determine the critical depth of erosion accurately. However, if the cumulative erosion on the front half of the island is examined as in Figure 11 a more accurate idea of critical depth effect is obtained.

The cumulative erosion for the profile corresponding to the radial which is perpendicular to the waves displays identical trends observed in cumulative erosion of the front half of the island. This would indicate a variation in cumulative erosion with scale and grain size is largely a two dimensional effect related to critical depth. There is a slight increase in cumulative erosion or critical depth from 200 to 100 scale and then a decrease to the 50 scale. Direct observation of critical depth also confirms it decreases with scale.

Kamphuis (1984) has adapted an equation developed by Hallermeier (1980) for initiation of sediment to describe the critical depth of erosion as follows:

$$H_c = K D^{1/4} T^{3/2} \sinh(kd_c) \quad [4.1]$$

where K is a constant and H_c is a wave height which yields critical depth d_c . The average value^c of K found in flume tests by Kamphuis was 0.12 and is identical to the average value of K for the island tests. This was somewhat fortuitous since the flume tests by Kamphuis were in fact in the middle range of the island tests (i.e. 100 scale). Both flume tests and island tests indicate critical depth is dependent on scale (or H^2/DL) and on grain size Reynolds number and therefore K is not a constant.

The significance of this scale effect would be illuminated if the critical depth in prototype were known. Kamphuis (1984) has fitted a straight line to field results collected by Swart (1974) resulting in the following relation.

$$K = 0.125 + 0.037 H \quad [4.2]$$

Using this equation for K , the following prototype critical depths are estimated for a wave with an 8 second period using Equation 4.1:

D	Wave Height (m)	K (Eq. 4.2)	Prototype	Laboratory	
			Critical Depth (m) (Eq. 4.2)	Critical Depth (m) 200 scale	Critical Depth (m) 50 scale
0.20 mm	3	0.24	7.6		
	4.75	0.30	10.5	10.0	8.0
	6.5	0.37	12.0	12.0	10.0

The prototype critical depths are very similar to those found in the laboratory. This may indicate that the scale effect from critical depth is small.

5.0 THE USE OF REGULAR WAVES

The present tests were performed with regular waves which consistently produced plunging breakers. This very simple artificial wave climate allows a better understanding of the physics involved, but also results in much greater erosion rates than in the prototype case of irregular waves. The regular wave model creates a condition where all waves break at the same point and where the point of maximum longshore current velocity closely coincides with the point of greatest agitation of the bed, resulting in maximum sediment transport rate. For irregular waves, part of the wave spectrum results in spilling breakers, the longshore current velocity distribution is spread over a longer distance perpendicular to the beach and each wave does not break at the point of maximum value of longshore current. Tests which are now underway with irregular waves show that the trough and bar formed by the longshore current as well as the bedform in the

trough are not as pronounced. Also the waves refract further around the island, critical depths remain virtually the same, sediment transport rate is smaller by a factor of 3 to 4 and time to a certain morphological stage is greater by a factor 2.

6.0 EXTRAPOLATION TO PROTOTYPE

6.1 The Scale Series

The inability to scale down grain size correctly results in the most pronounced scale effect in coastal mobile bed models (Kamphuis 1982, 1975a). A complete understanding of this effect is very difficult because of incomplete theoretical understanding of the sediment transport mechanisms which involve sediment suspension, liquefaction of the bed, percolation and aeration of the surf zone. Also viscous and bedform effects introduce further complexities which are not fully understood. The results from a single physical model test of a previously untested coastal feature cannot therefore reliably describe a prototype e.g. how would one extrapolate from one single point in Figures 6, 7 or 8? One option remaining (until scale effect is fully understood) is a series of tests at different scales. The philosophy of the series of tests is to provide some understanding of the influence of scale effects in the range of scales tested as evidenced by Figures 6, 7 and 8 in the present tests and with this knowledge, attempt to extrapolate to prototype.

6.2 Validity of Extrapolation

The present series of tests has revealed the erosion (or sediment transport) rates of the front half of the island for model scales 200 to 50. Any attempt at extrapolation cannot be entirely dependable. However, in some cases extrapolation may be attempted with more confidence than others, for instance extrapolation of the 0 to 3 hr prototype time period (Figure 6A) or the morphological stage to the post, Figures 7 and 8, would be more reliable than longer prototype time periods, (Figures 6B and C) where curvature and differences between the lines of various grain sizes is much more severe. During the shorter prototype time period differences between erosion rates for different grain diameters are not large and the use of smaller grain sizes than the prototype sand aid in extrapolation because the values of H^2/DL for the finer sands will be greater and closer to the prototype value. It is apparent that the prototype grain diameter should be used in models if longer morphological time segments are used in the extrapolation because of the critical depth effect resulting from differing diameters is large (Figure 8).

Vellinga (1982, 1978) carried out a series of two dimensional dune erosion tests at different scales and grain diameters. In order to establish scaling relationships (based on the fall velocity parameter H/Tw) Vellinga built models with different profile distortions and it was discovered that distortion was directly proportional to erosion. Therefore, Vellinga's results can be plotted using the parameters of the present paper by dividing the erosion quantity for a test by the initial profile distortion from a

prototype. The plots for three prototype time periods are shown in Figures 12A, B and C and these figures show the same trends observed for the island tests i.e. the longer time periods show more curvature and a greater difference between the different grain diameters. Vellinga's 5 hr prototype results were enhanced by a test at scale 5 in the Delta flume at Delft. These results have been plotted in Figure 12A and demonstrate that extrapolation is not outside the realm of consideration for shorter prototype time periods.

6.3 Extrapolation of Results

An attempt was made at extrapolation using two methods, extrapolating the dimensionless erosion rate for a short prototype time period and extrapolating over a morphological time segment. These two methods were employed to determine the time for the erosion scarp to reach the post at the centre of the island. For the first method an erosion rate was determined for 0 to 3 hrs for the prototype by extrapolation of Figure 6A. The second method was a direct extrapolation of the time to the post (Figure 8). The following results were obtained for regular waves with an 8 second period:

H(m)	time to reach the post (hrs)	
	method 1	method 2
6.5	2-3	3-6
4.75	3-5	5-10

The credibility of extrapolation is demonstrated by the fact that these separate methods yield results of the same magnitude.

The erosion of one prototype island in the Beaufort Sea was monitored by Esso Resources Canada with aerial photographs over the period of three storms in October 1980. During these storms which each lasted less than a day and featured significant wave heights of about 3 m and a wave period of 7 s the island was eroded from the edge of the drilling platform at the top of the 1 in 3 slope to approximately the centre of the island. It is estimated that each storm lasted about 6 hrs, hence the island was effectively subjected to approximately 18 hrs of waves with an approximate significant wave height of 3 m and period of 7 seconds. The extrapolation of model results with 3 m wave height and 8 second period for the morphological time period from the top of the 1:3 slope to the post yield an erosion time of 8 hours for the prototype. Since it was discovered in the model tests with irregular waves that the progression of erosion with the regular wave tests was about twice that with irregular waves, the above number needs to be doubled, giving an approximate estimated prototype erosion time of 16 hours. It must be stressed that both the prototype data and the extrapolation from the models are very approximate but the above comparison looks very promising.

7.0 CONCLUSIONS AND RECOMMENDATIONS

1. Scale effects are mainly due to the incorrect simulation of grain diameter.

2. The change in sediment transport rate with scale is primarily due to inertial effects.

3. Viscous effects and the existence of bedform and critical depth scale effects cause secondary influences which make direct extrapolation difficult.

4. To model a previously untested coastal feature, a series of tests must be performed which provides a basis for extrapolation of results to prototype.

5. The influences of the various scale effects have been identified within the scale series but their role in the zone of extrapolation is still relatively unknown. Further research is required at smaller scales.

6. Extrapolation can be performed with some degree of confidence for short prototype time periods and for morphological time segments.

7. Critical depth effects become large between different model grain diameters for the longer prototype times and extrapolation can only effectively be performed from models with the prototype grain size. Over short prototype time periods profile evolution and erosion rates are not much different for the different scales and extrapolation from different grain size curves is possible. Since critical depth effects are minimal in the early time periods finer grain sizes than prototype would help to close the gap on extrapolation to the prototype value of H^2/DL .

8. At lower values of H^2/DL or H/D (Sawaragi and Deguchi suggest a limit of $H/D = 300$) sediment transport will be mainly by bed load in the laboratory and will not resemble a prototype which features predominant suspended load.

8.0 ACKNOWLEDGEMENTS

The work presented in this report was supported financially by a grant from the Natural Sciences and Engineering Research Council of Canada (NSERC). The junior author was also supported by an NSERC scholarship during his study at Queen's. The actual model testing involved many individuals and the authors are grateful for the support by this team of dedicated people.

9.0 REFERENCES

1. Hallermeier, R.J. (1980) "Sand Motion Initiation by Water Waves: Two Asymptotes", Journal of Waterway, Port, Coastal and Ocean Division, ASCE, Vol. 106, WW3, Aug 1980 pp. 299-318.
2. Kamphuis, J.W. (1975) "Friction Factor Under Oscillatory Waves", Journal of the Waterways, Harbours and Coastal Engineering Division, ASCE, Vol. 101, WW2, May 1975, pp 135-144.
3. Kamphuis, J.W. (1975) "The Coastal Mobile Bed Model", Queen's University Civil Engineering Research Report No. 75, 113 pp.
4. Kamphuis, J.W. (1982) "Coastal Mobile Bed Modelling from a 1982 Perspective", Queen's University Civil Engineering Research Report No. 76, 38 pp.
5. Kamphuis, J.W. (1984) "The Erosional Process along a Till Shoreline", unpublished report to the Deputy Attorney General of Canada, pp. 22-87.
6. Komar, P.D. and Miller, M.C. (1974) "Sediment Threshold Under Oscillatory Waves", Proceedings of the 14th International Conference on Coastal Engineering, Copenhagen 1974, pp. 756-775.
7. Madsen, O.S. and Grant, W.D. (1976) "Quantitative Description of Sediment Transport by Waves", Proceedings of the 15th International Conference on Coastal Engineering, Honolulu 1976, pp. 1093-1112.
8. Mogridge, G.R. (1974) "Scale Laws for Bedforms in Laboratory Wave Models", Proceedings of the 14th International Conference on Coastal Engineering, Copenhagen 1974, pp. 1669-1085.
9. Sawaragi, T. and Iwata, K. (1974) "On Wave Deformation after Breaking", Proceedings of the 14th International Conference on Coastal Engineering, Copenhagen 1974, pp. 481-497.
10. Sawaragi, T. and Deguchi, I. (1978) "Distribution of Sand Transport Rate Across a Surf Zone", Proceedings of the 16th International Conference on Coastal Engineering, Hamburg 1978, pp. 1596-1613.
11. Sayao, O.F.S.J. (1982) "Beach Profiles and Littoral Sand Transport", Ph.D. Thesis, Department of Civil Engineering, Queen's University.

12. Swart, D.H. (1974) "Offshore Sediment Transport and Equilibrium Beach Profiles", Delft Hydraulics Laboratory Publication No. 131, pp. 302.
13. Vellinga, P. (1978) "Moveable Bed Tests on Dune Erosion", Proceedings of the 16th International Conference on Coastal Engineering, Hamburg 1978, pp. 2020-2039.
14. Vellinga, P. (1982) "Beach and Dune Erosion During Storm Surges", Coastal Eng., 6:361-387.

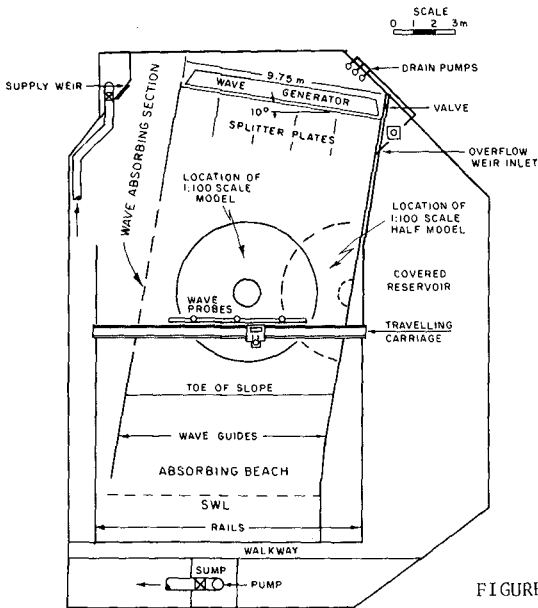


FIGURE 1: MODEL BASIN

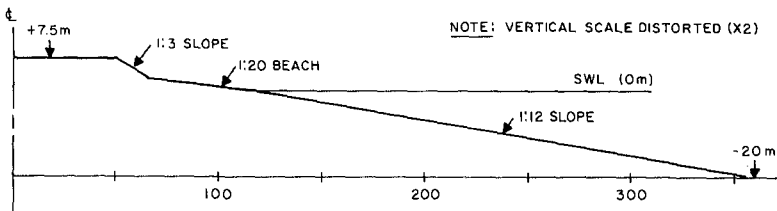
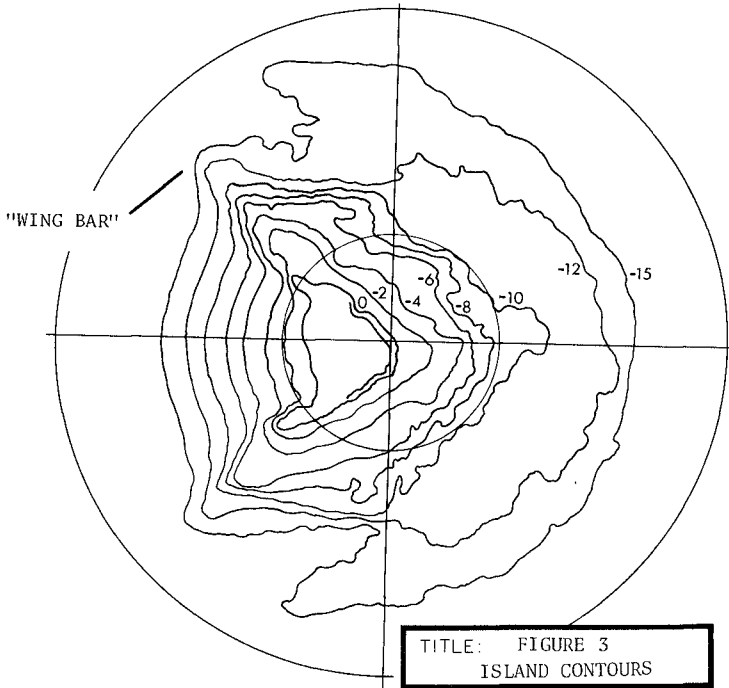
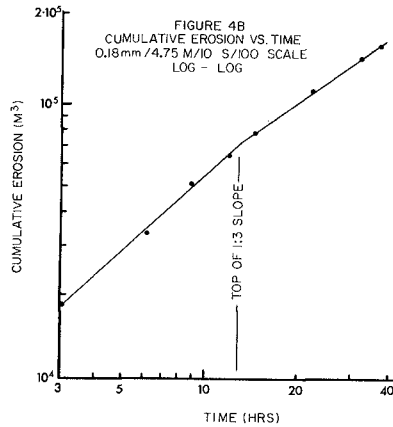
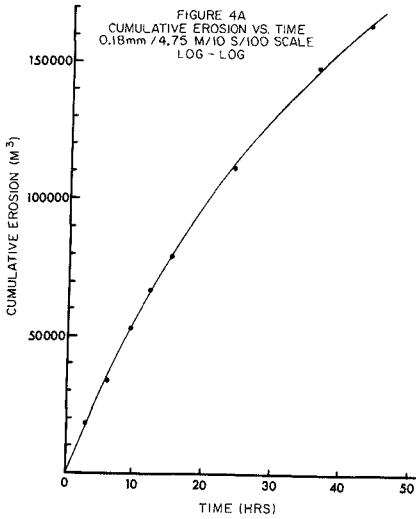


FIGURE 2: PROTOTYPE ISLAND PROFILE



TITLE: FIGURE 3	
ISLAND CONTOURS	
SCALE: 1:100	H: 6.5 m.
TIME: 40 HRS	T: 8 SECS.
D ₅₀ : 0.105 MM	



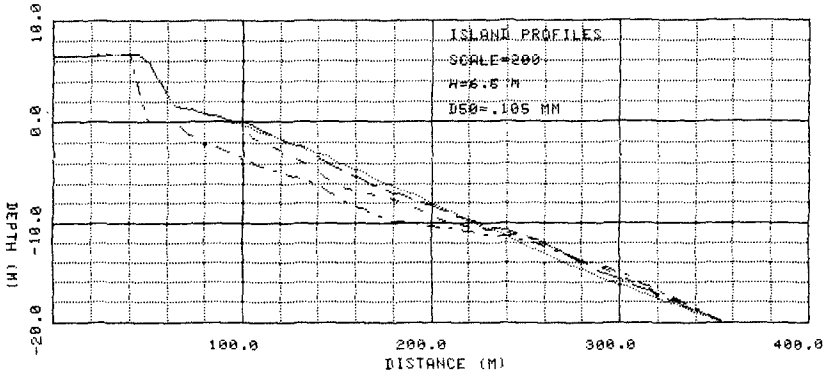
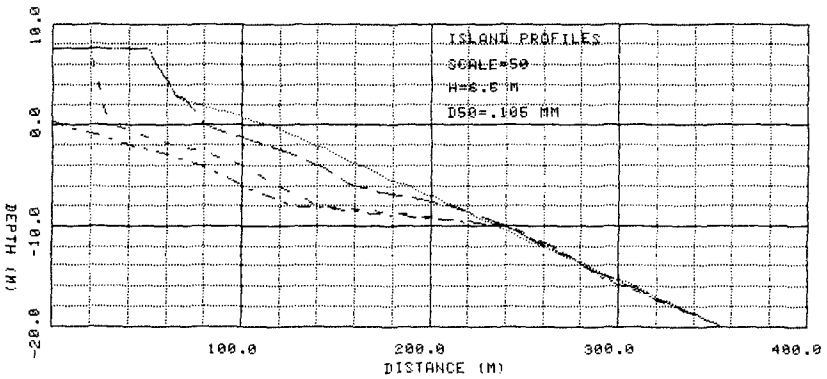


FIGURE 5 A, B: ISLAND PROFILES AT 0, 3, 12, 36 HRS. OR POST



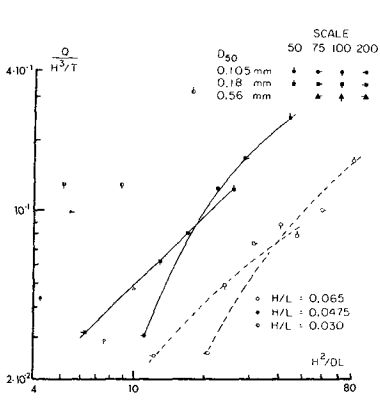


FIGURE 6A: DIMENSIONLESS EROSION VS. H^2/DL
0-3 HRS. LOG-LOG

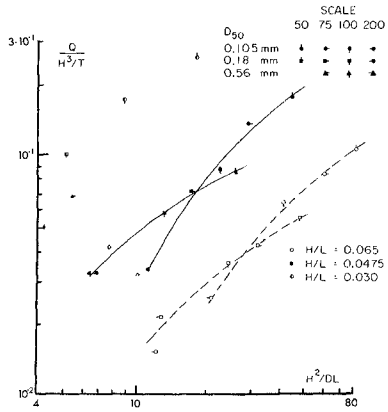


FIGURE 6B: DIMENSIONLESS EROSION VS. H^2/DL
0-12 HRS. LOG-LOG

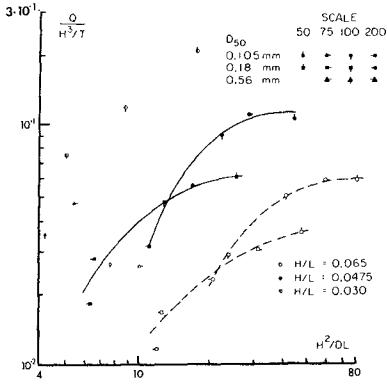


FIGURE 6C: DIMENSIONLESS EROSION VS. H^2/DL
0-36 HRS. LOG-LOG

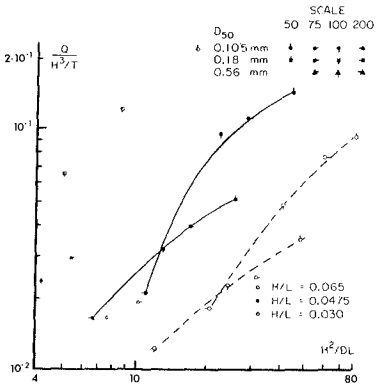


FIGURE 7: DIMENSIONLESS EROSION VS. H^2/DL
0 HR. TO THE POST LOG-LOG

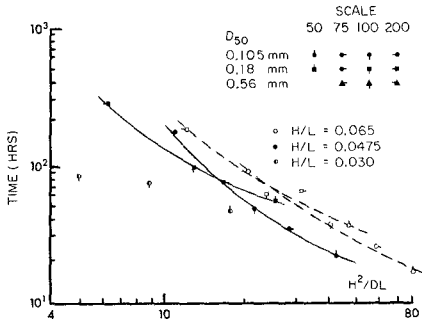


FIGURE 8: TIME TO REACH THE POST VS. H^2/DL LOG-LOG

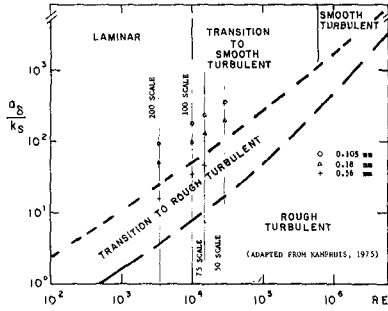


FIGURE 10: FLOW REGIMES

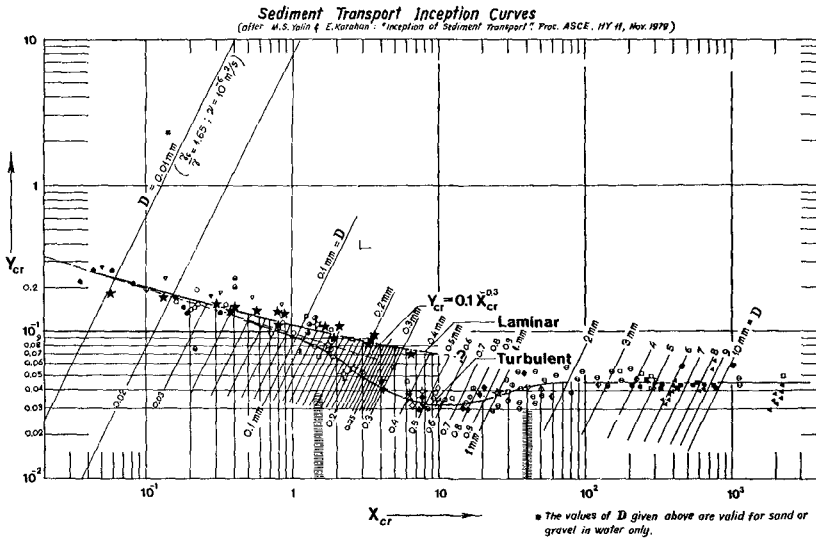


FIGURE 9: SHIELDS DIAGRAM

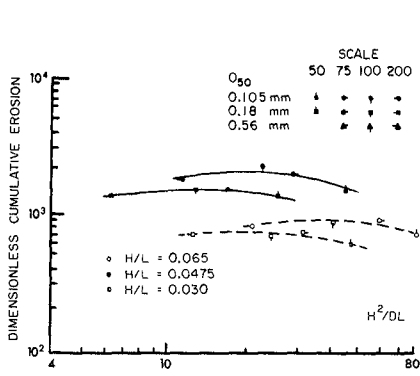


FIGURE 11: DIMENSIONLESS EROSION VS. H^2/DL 0 HR. TO THE POST LOG-LOG

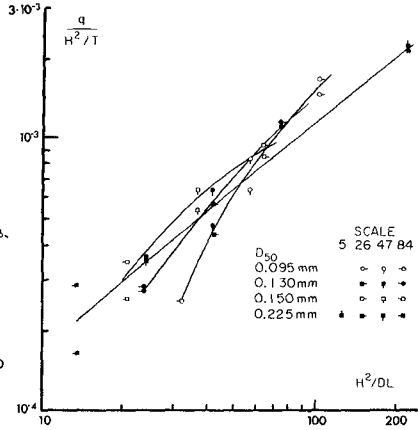


FIGURE 12A: DIMENSIONLESS EROSION RATE VS. H^2/DL VELLINGA DATA 0 TO 5 HRS. PROTOTYPE

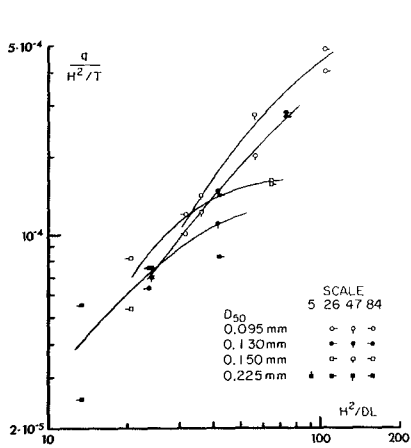


FIGURE 12B: DIMENSIONLESS EROSION RATE VS. H^2/DL VELLINGA DATA 0 TO 30 HRS. PROTOTYPE

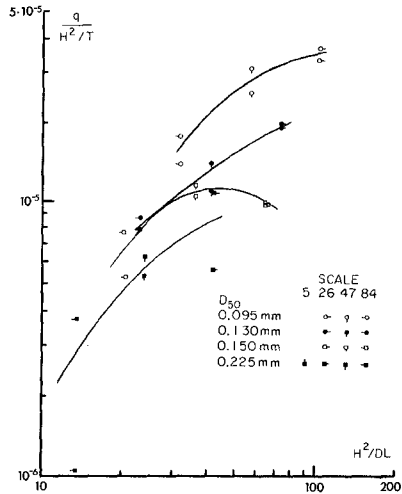


FIGURE 12C: DIMENSIONLESS EROSION RATE VS. H^2/DL VELLINGA DATA 0 TO 100 HRS. PROTOTYPE